Desalination and Water Treatment
www.deswater.com
doi: 10.5004/dwt.2022.28421

258 (2022) 123–132
May

Competitive adsorption of Zn in wastewater effluents by NaOH-activated raw coffee grounds derivative and coffee grounds

Najat Qisse[a], Ghizlane Fattah[b], Mohamed Elouardi[a], Jamal Mabrouki[a,*], Laila El azzouzi[a], Abdelali Ennouari[b], Mohammed Alaoui El Belghiti[a], Mohamed EL Azzouzi[a]

[a]*Laboratory of Spectroscopy, Molecular Modeling, Materials, Nanomaterial, Water and Environment, CERNE2D, Mohammed V University in Rabat, Faculty of Science, Avenue IbnBattouta, BP1014, Agdal, Rabat, Morocco, email: jamal.mabrouki@um5r.ac.ma (J. Mabrouki)*
[b]*Civil, Hydraulic and Environmental Engineering Laboratory, Mohammadia School of Engineers, Mohammed V University, Avenue IbnSina B.P 765, Agdal Rabat,10090 Morocco*
[c]*Depatement of Biology, Mohammed V University in Rabat, Faculty of Science, Avenue IbnBattouta, BP1014, Agdal, Rabat, Morocco*

Received 20 October 2021; Accepted 21 March 2022

ABSTRACT

Heavy metal pollution has become a pressing environmental issue. The removal of these metals from the environment is a considerable concern because of their effects. In this study, we have used wastewater to assess the adsorption properties of Zn^{2+} using NaOH-activated carbon (raw coffee grounds derivative (CGD)). We also compared the adsorption performance of Zn^{2+} by coffee grounds (CG) and NaOH-activated CGD biochars. In addition, we have carried out characterization to determine the adsorbent' physico-chemical properties. Therefore the results indicated that the pseudo-second-order model and all isotherm models were the most adequate to describe Zn(II)/activated carbon adsorption system. Also, the NaOH-activated carbon has shown a high adsorption capacity of about 680.2 μmol g^{-1} compared to coffee grounds (CG) (300.51 μmol g^{-1}).

Keywords: Adsorption; Heavy metals; Wastewater; NaOH-activation; Coffee grounds

1. Introduction

Heavy metals are present a highly toxic impact on the ecosystem, above a specific concentration [1–3]. They can be accumulated in the food chain, hence in the human body [4]. Industrial activities such as battery production, electronics, ceramics, metal processing, textiles, petroleum refining and many others are the principal sources of heavy metals in wastewater [5–7]. Consequently, it is essential to reduce these pollutants from wastewater. To remove these toxic elements from wastewater, several pollution techniques have been developed in recent years. Among these techniques used, integrated chemical/biological degradation, membrane technology, chemical oxidation, electrochemical degradation, photocatalytic degradation and adsorption [8–15]. Among these technologies, the adsorption method is a cost-effective and efficient technique for removing heavy metals from wastewater [16]. Several adsorbents are applied in this context like materials based on carbon [17,18], zeolites [19], clay [20], and graphene oxide [21]. Among these adsorbents, we found also activated carbon, which is the most used for the treatment of this kind of pollutants, due to its large specific surface area and porous structure [22]. Wood [23] and peat [24] are the most common sources for producing commercial activated carbons. Nevertheless, the need is increasing

* Corresponding author.

for efficient materials, locally available and recyclable that could be used to prepare activated carbon [25–27]. Converting biomass resources into activated carbons is a practical method for producing low cost and efficient carbon-based adsorbents. Coffee wastes are an available, abundant and inexpensive raw material that after processing into activated carbons can be effective to remove heavy metals from wastewater. There are a considerable number of research work that studied the efficiency of the raw and treated coffee ground for the elimination of heavy metals such as Cu(II) and Zn(II) [28], Cd^{2+} [29], Cu(II), Pb(II), Cd(II), Ni(II) and Zn(II) [30]. The coffee grounds are a significant source of solid pollution. Therefore, the exploitation of these materials in wastewater treatment will generate economic and ecological benefits. In this context, we will study the efficiency of the ground coffee and activated carbon based on the ground coffee to eliminate heavy metals from the effluents. Furthermore, to upgrade their adsorption proprieties and to conserve the cost-efficiency ratio we will study the impact of the activation using NaOH.

Finally, we will investigate and discuss the performance of our adsorbents to remove Zn^{2+} metal ions from wastewater. We will also carry out kinetic and isotherm studies to have an overview of the adsorption phenomenon.

2. Materials and methods

2.1. Materials

2.1.1. Chemicals

Based on the literature sodium hydroxide has been widely used for chars activation [11]. The feedstock (ground coffee) was placed in a horizontal stainless steel furnace and heated to 500°C under nitrogen flow with a heating rate of 20°C min^{-1} and then conserved for 2 h at 500°C. The 10 g of the charcoal was obtained by carbonization was mixed with 20 g of NaOH and 100 mL of distilled water. The mixture was stirred for 2 h then put in the oven for 4 h at 130°C. The resulting product was then placed in the calcination furnace, under nitrogen flow up to 700°C with a heating rate of 20°C min^{-1} for 1.5 h. The obtained material was washed with a solution of hydrochloric acid (0.1 M), then with hot distilled water until the pH of the supernatant becomes 6.5, the final product was dried at 110°C for 24 h [10].

2.1.2. Collection of lake water and wastewater effluent

The samples used in this work were collected from an industrial wastewater treatment plant located in (name the city). The effluent has a yellow colouration, with a strong smell because of the presence of the surfactants and hydrocarbons. All the effluent characteristic parameters were measured including pH, chemical oxygen demand (COD), biochemical oxygen demand (BOD_5), total Kjeldahl nitrogen (TKN), total suspended solids (TSS), and total phosphorus (TP).

2.1.3. Biochar production procedures

The dried raw coffee grounds derivative (CGD), with a particle size smaller than 250 μm, was placed in a stainless-steel furnace and heated at a rate of 15°C min^{-1} at 450°C. After 2 h of heating, the carbonized material obtained was gradually cooled. Then, the carbonized material was activated by mixing with NaOH at a weight ratio of 2:1 (NaOH: Carbonized material). The mixture was placed in a stainless-steel reactor and heated under nitrogen at a rate of 15°C min^{-1} at 450°C and maintained at a contact time of 60 min. Then the mixture was cooled under nitrogen flow and then washed several times with deionized water and a diluted solution of HCl until the pH of the filtrate reached a value of 7. The obtained NaOH-activated biochar was dried at 110°C overnight [31].

2.2. Methods

2.2.1. Characterisations of coffee grounds

2.2.1.1. Scanning electron microscopy characterization

The scanning microscopic characterization of coffee grounds and activated carbon based on coffee grounds was carried out using a scanning electron microscope, GEOL JSM T330, in the Physics Department of the Faculty of Sciences, Rabat.

2.2.1.2. Specific surfaces area measurement

The specific surface measurements were made using an ASAP 2010 micrometre in Mascir laboratory, Morocco. The degassing of the samples was carried out at 250°C under a mixture of He (70%) and N_2 (30%) for 2 h. The measurements were repeated to ensure reproducibility.

2.2.1.3. Infrared spectroscopy analysis

The device used for this is a Bruker-Tensor 27 that operates in Reflection mode. This device is equipped with a Globar source that emits radiation in the mid-infrared region and a DLaTGS detector. The samples do not require any prior preparation. A few milligrams of the sample are placed on the Attenuated Total Reflection (ATR) element. The material used in our case is the Germanium crystal which allows the acquisition of between 4,000 and 600 cm^{-1} in wavenumber. The number of scans is 20 with a resolution of 4 cm^{-1}. The device is generally controlled by OPUS software.

2.2.2. Batch adsorption tests

All experiments were performed using 0.1 g of adsorbent in 50 mL of wastewater sample in an Erlenmeyer flask. The mixture was stirred at 150 rpm for 3 h. For each experiment, samples were collected in glass bottles cleaned before and after adsorption for analysis.

2.2.3. Kinetic adsorption

To examine the adsorption mechanism, it is necessary to test the experimental adsorption data using pseudo-first-order and pseudo-second-order kinetic models.

The pseudo-first-order model assumes that the adsorption rate at time t is proportional to the difference between the amount adsorbed at equilibrium Q_e and the amount Q_t

adsorbed at that time. The first-order adsorption rate constant is derived from the linear model [32].

$$\log\left(Q_e - Q_t\right) = \log\left(Q_e\right) - \frac{k_1}{2{,}303}t \tag{1}$$

where Q_e: amount of adsorbate at equilibrium, per gram of adsorbent (mg g^{-1}), t: contact time (min), and k_1: first-order adsorption rate constant (min^{-1}).

The pseudo-second-order equation is often used successfully to describe adsorption kinetics. It assumes that the adsorption is of the chemical type [33].

$$\frac{t}{Q_t} = \frac{1}{\left(k_2 \cdot Q_e^{\,2}\right)} + \frac{1}{Q_e}t \tag{2}$$

The linear equation [34] for intraparticle diffusion is shown in Eq. (3):

$$q_t = k_p \cdot t^{0.5} + C \tag{3}$$

where k_p (mg g^{-1} $min^{-0.5}$) are rate constants and C is a constant.

2.2.3.1. Protocol

To study the adsorption kinetics of Zn^{2+} ions, we put a volume of 100 mL of water discharged in a batch to which we add 0.15 g of NaOH-activated CGD biochar. Samples of the supernatant of the mixture (adsorbate/adsorbent) are taken every 10 min then they were filtered using a nylon membrane (0.22 μm). The final concentration of Zn^{2+} ions is measured for each sample.

2.2.4. Adsorption isotherms

In order to describe the characteristics of an adsorbent/adsorbate system, several theoretical and empirical models have been developed. The isotherm of Langmuir, Freundlich and Temkin, is the most widely used model in the adsorption process.

The empirical equation given by Langmuir [35] is represented by the equation:

$$\frac{1}{Q_e} = \frac{1}{Q_m} + \frac{1}{\left(Q_m \cdot k_L \cdot C_e\right)} \tag{4}$$

with Q_m and Q_e which are respectively the maximum amount of adsorption (mg g^{-1}) and the amount of adsorption at equilibrium (mg g^{-1}), this is the concentration of the solute at equilibrium (mg L^{-1}), and k_L is Langmuir's constant (L mg^{-1}).

The Freundlich equation [36] is an empirical model based on adsorption on heterogeneous surfaces. It is used in the case of the possible formation of more than one adsorption monolayer on the surface and the sites are heterogeneous with different binding energies. The isotherm is expressed by the linear equation: k_F and n are constants that depend respectively on the nature of the adsorbate and of the adsorbent. Their determination is based on the following equation:

$$\log\left(Q_e\right) = \log\left(k_F\right) + \frac{1}{n}\log\left(C_e\right) \tag{5}$$

This equation is that of a straight line with slope $1/n$, and ordinate at the origin $\log k_F$. In general, n is between 0.8 and 2 and is proportional to the strength of the adsorption.

Temkin's model [37] assumes that the heat of adsorption varies linearly with the degree of coverage, this variation may be related to surface heterogeneity or side interactions between adsorbed molecules.

$$q_e = B_T \ln K_T + B_T \ln C_e \tag{6}$$

where B_T = constant related to heat of sorption (J mol^{-1}) $B_T = RT/b_T$ and b_T = Temkin isotherm constant.

Another equation used in the analysis of isotherms was proposed by Dubinin and Radushkevich in 1947. By Dubinin and Radushkevich in 1947 to estimate the characteristics of the apparent porosity and the free energy of adsorption.

$$\ln Q_e = \ln Q_m - \beta\varepsilon^2 \tag{7}$$

where Q_m the theoretical maximum capacity of the adsorbate at the surface of the solid and ε, the Polanyi potential, corresponding to:

$$\varepsilon = RT \ln\left(1 + \left(\frac{1}{C_e}\right)\right) \tag{8}$$

The constant β represents the adsorption of the molecule on the adsorbent following its transfer from the solution. β and E (kJ mol^{-1}) are related by the relation $E = 1/\beta^{0.5}$.

2.2.4.1. Protocol

The adsorption isotherms were carried out with different samples of wastewater containing different concentrations of Zn^{2+} at solution pH and room temperature for a fixed time (equilibrium time). After stirring, the mixture was centrifuged for 20 min to isolate the NaOH-activated CGD biochar particles. The filtrates were analyzed by atomic absorption to determine the residual Zn^{2+} concentration in the solutions.

2.2.5. Thermodynamic study

The enthalpy change ($\Delta H°$) and the entropy change ($\Delta S°$) were estimated to assess the feasibility of the adsorption process by the following equations [38]:

$$\Delta G° = -RT \ln\left(k_d\right) \tag{9}$$

$$\ln\left(k_d\right) = \frac{\Delta S°}{R} - \frac{\Delta H°}{RT} \tag{10}$$

where k_d is the distribution coefficient for the adsorption, R is the universal gas constant (8.314 J mol^{-1} K^{-1}) and T is the absolute temperature (K).

2.2.5.1. Protocol

The thermodynamic parameters linked to the adsorption phenomenon were also determined by varying the temperature of the solution from 303 to 353 K.

2.2.6. Analytical methods

The samples before and after treatment were analyzed by the atomic absorption spectrophotometer. Before analysis, all samples were homogenized and filtered through glass filters. The heavy metals removal percentage was calculated using the following formula [39].

$$\text{Removal}\% = \frac{C_i - C_e}{C_e} \times 100 \quad (11)$$

where C_i is the initial concentration at equilibrium (ppm) and C_e is the final equilibrium concentration (ppm).

3. Results and discussion

3.1. Physico-chemical characterization

The evaluation of wastewater pollution was based on the determination of several physico-chemical parameters that characterize the wastewater quality. The physico-chemical characteristics of the studied wastewater are listed in Table 1. The wastewater temperature is between 28°C and 26°C respectively minimum and maximum extreme values (Table 1). In general, the wastewater samples analyzed have a relatively acceptable pH.

For electrical conductivity, the average values recorded are 11.1 and 2.5 mS cm^{-1} respectively for the raw and the treated wastewater, which shows a high metal load. For the phosphate content, the data in the table does not show a remarkable variation before and after the treatment. The values recorded are 9 and 5 mg L^{-1} respectively before and after treatment. The phosphate concentrations for the treated wastewater showed that these raw effluents are loaded with phosphate. (Table 1). The wastewater TSS concentration is about 65 mg L^{-1}. The organic pollution expressed as BOD_5 show a value of 212 mg L^{-1}. And the COD values show a value of 842 mg L^{-1} (in raw wastewater) and 419.52 mg L^{-1} in treated wastewater (Table 1).

3.2. Characterization of coffee grounds and NaOH-activated CGD biochars

3.2.1. Specific surface analysis

The characterization of the specific surface by the method of Brunauer–Emmett–Teller (BET) aims to determine the adsorbent's surface area. The results of the surface analysis are shown in Table 2.

Table 2 shows that the activation treatment improves the pore volume. NaOH-activation can dissolve some of the inorganic compounds that block the pores. Consequently, the pores became available and more pores are formed. The increase in the number of pores leads to an increase in adsorption efficiency.

The results of the BET test show that the average pore diameter of coffee grounds was 7.6 Å while NaOH-activated CGD biochar was 8.8 Å.

3.2.2. Fourier-transform infrared spectroscopy analysis

Fourier-transform infrared spectroscopy (FTIR) characterization aims to see the functional groups contained coffee grounds and NaOH-activated CGD biochar. Fig. 1

Table 1
Characterization of the studied wastewater before and after treatment

Parameters	Raw wastewaters	Treated wastewater	Moroccan standard
T (°C)	28	22	<30
pH	8.8	8.1	5.5–9.5
Conductivity (mS cm^{-1})	11.1	2.5	2.7
TSS (mg L^{-1})	65	5.2	50
COD (mg L^{-1})	842	542	500
BOD_5 (mg L^{-1})	212	34	140
TKN (mg L^{-1})	50	14	30
P (mg L^{-1})	9	5	10
Metals			
Fe (mg L^{-1})	5.1	1.6	5
Zn (mg L^{-1})	11.3	5.8	5
Cu (mg L^{-1})	10.4	0.4	0.5
Cd (mg L^{-1})	0.12	0.014	0.25
Pb (mg L^{-1})	0.09	0.016	0.5
Colour (Absorbance)			
430 (nm)	18	0.002	–
536 (nm)	16.7	0.002	–

Table 2
Surface area result of CG and NaOH-activated CGD biochar

Adsorbent type	Specific surface ($m^2\ g^{-1}$)	Pore volume ($cm^3\ g^{-1}$)	Pore size (Å)
Coffee grounds (CG)	60.3	0.039	7.6
NaOH-activated CGD biochar	664.2	0.468	8.8

shows the coffee grounds and NaOH-activated CGD biochar infrared spectra according to bibliographic results.

The functional group and the corresponding infrared absorption frequencies are shown in Table 3.

FTIR spectroscopic analysis showed a band at 3,472 cm^{-1} representatives bound to OH or NH groups on the surface of the coffee grounds. The peaks at 2,924 and 2,853 cm^{-1} are related to C–H vibrations, so the adsorption peaks at 1,746 cm^{-1} are attributed to the resulting carboxyl bond of the xanthenic derivative such as caffeine [40]. The absorption bands at 1,467 at cm^{-1} respectively indicate the presence of COO of the carboxyl groups on the surface of the adsorbent. Bands of the order of 1,378 cm^{-1} are attributed to the symmetrical stretching vibration COO−. Another absorption band appearing around 1,168 and 1,030 cm^{-1} could be attributed to the C–O stretch of the ether group and the C–O stretch of COOH [41]. On the other hand, for the spectrum of NaOH-activated CGD biochar, we observed the presence of adsorption peaks at 3,430; 1,565; 1,384 and 1,213 cm^{-1}. While the adsorption peaks at 2,924; 2,853; 1,746 and 1,030 cm^{-1} are resolved after pyrolysis and activation with sodium hydroxide. This shows that the activation process affects the intensity of absorption in the wavelength region and results in changes in the structure of the functional group [42].

3.2.3. Physico-chemical properties of coffee grounds and NaOH-activated CGD biochars

Fig. 2 shows the adsorbents morphology before and after activation. Activation with NaOH significantly has caused variation in the biochar morphology by developing several pores and increasing the pore volumes, as shown in the scanning electron microscopy (SEM) images. Therefore, increase the metal ion adsorption.

The physico-chemical characteristics of coffee grounds (CG) and NaOH-activated CGD biochar are presented in Table 4. Although the specific surface area (664.2 $m^2\ g^{-1}$) and the pore volume (0.468 $cm^3\ g^{-1}$) of NaOH-activated CGD biochar are much higher than those of CG (specific surface area = 60.3 $m^2\ g^{-1}$, pore volume = 0.039 $cm^3\ g^{-1}$), the average pore size of CG (7.6 nm) was less than that of NaOH-activated CGD biochar (mean pore size = 8.8 nm). These results suggest that mesoporous structures could

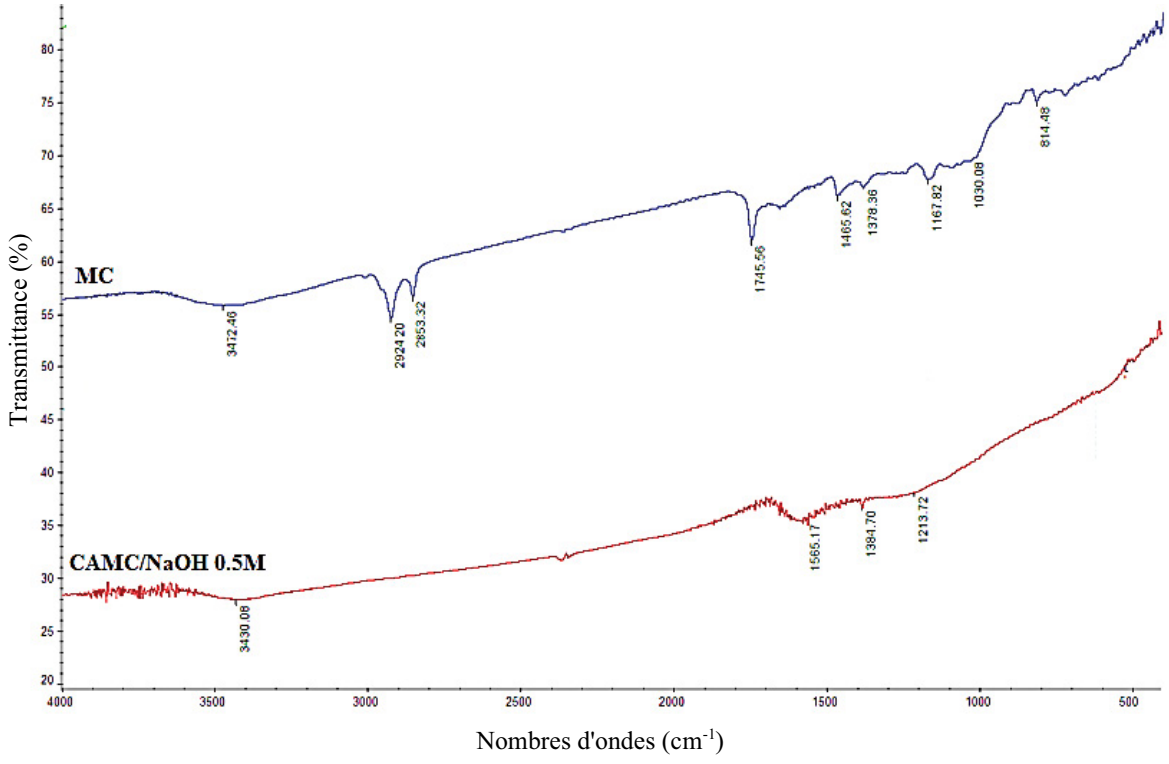

Fig. 1. FTIR spectrum for adsorbent of coffee grounds and NaOH-activated CGD biochar.

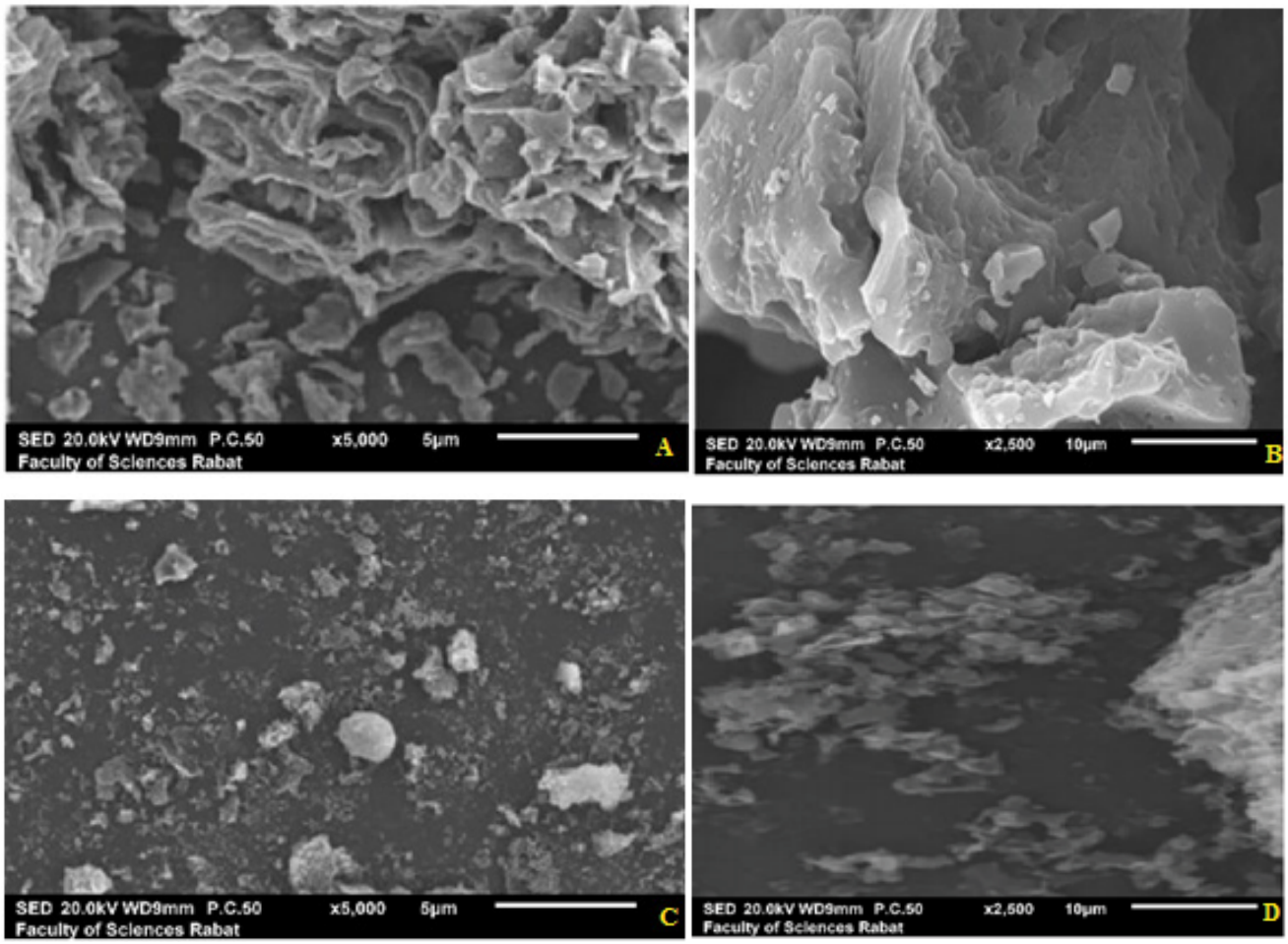

Fig. 2. The UHR-SEM images of the (A,B) coffee grounds and (C,D) NaOH-activated CGD biochars.

Table 3
CG and NaOH-activated CGD biochar infrared spectrum

Plage	Wavenumber (cm^{-1})	
Bond	Coffee grounds	NaOH-activated CGD biochar
OH and NH	3,472	3,430
C–H	2,924	–
C–H_2	2,853	–
C=O	1,746	–
COO	1,467	1,565
COO–	1,378	1,384
C–O	1,168	1,213
C–O and COOH	1,030	–

play a critical role in the adsorption of Zn^{2+} by NaOH-activated CGD biochar and CG. The C, H, N, O and ash contents of biochar CG and NaOH-activated CGD biochar are summarized in Table 4. NaOH-activated CGD biochar contained C (88.2%) and ash (6.8%) lower than those of CG (C content = 85.1%, ash content = 7.2%) while its H (0.7%) and N (2.2%) contents were slightly higher than those of NaOH-activated CGD biochar (H content = 0.4%, and their N content is not detected).

3.3. Adsorption kinetics

The biochar shows an increase in the adsorbed quantity Q_{ads} over time. A rapid increase in the first 10 min was noticed for the 2 studied adsorbents, then a slight increase was observed. The equilibrium time of 120 min was observed for the NaOH-activated CGD biochar and 20 min for coffee grounds. We can explain the Q_{ads} stabilization by the saturation of the active sites in the adsorbent's surface. Also, we can deduce from Fig. 3 that Zn^2 is strongly adsorbed on the CG compared to NaOH-activated CGD biochar.

3.3.1. Kinetic models

Kinetic models were used to study the experimental data shown in Fig. 4 to obtain the kinetic parameters (Table 5). As shown in Table 5, the pseudo-second-order kinetic model showed a higher correlation coefficient value which indicates that the Zn(II) adsorption experiment data is fit to this model. Fig. 3 also shows that the theoretical

Table 4
Elemental composition and physico-chemical properties of the coffee grounds and NaOH-activated CGD biochars

Properties	Coffee grounds (CG)	NaOH-activated CGD biochar
C (%)	85.1	88.2
H (%)	0.7	0.4
O (%)	1.6	2.2
N (%)	2.2	N.D.
S (%)	0.4	0.2
Ash (%)	7.2	6.8
H/C	0.118	0.035
O/C	0.014	0.038
N/C	0.021	N.A.

value of the adsorption capacity of coffee grounds (CG) adjusted by the pseudo-second-order model is closer to the experimental data of Q_e. The diffusion mechanism cannot be determined by the pseudo-second-order and pseudo-first-order kinetic models. Therefore, an in-depth analysis of dynamic behaviour using the intraparticle diffusion model is required. The value (R^2 < 1) fitted by the intraparticle diffusion model proves that the fitted line does not pass the origin; thus, intraparticle diffusion occurred during the adsorption process [43]. In addition, as shown in Fig. 4, the intraparticle diffusion model comprises two adjustment steps [44]. The first adjustment step indicates the diffusion of Zn(II) on the surface or membrane of the NaOH-activated CGD biochar adsorbent during the adsorption process. The second-step had a flat linear part, which indicates the diffusion of Zn(II) into the particles or pores of NaOH-activated CGD biochar. The curved part can be the boundary layer effect that occurs during the adsorption process. Therefore, the adsorption of Zn(II) on NaOH-activated CGD biochar is affected in two ways: chemical adsorption and intraparticle diffusion.

Intraparticle diffusion is normally studied to understand the diffusion mechanism of an adsorbate on a porous adsorbent such as biochar. The transfer of adsorbed ions inside the biochar particles is called intraparticle diffusion (also called surface diffusion). Thus, the model of Weber and Morris was used to illustrate the Zn^{2+} ions adsorption process on biochar, by plotting Q_t vs. $t^{1/2}$. If the trace is linear and passes through the origin, intraparticle diffusion is then the only limiting step of the adsorption process [45]. However, since the trace does not pass through the origin, the adsorption process is therefore produced in several steps.

The intraparticle diffusion of Zn^{2+} adsorbed on the NaOH-activated CGD biochar was presented in (Fig. 4). The initial increase (Fig. 4) during the first 60 min (approximately 7.5 $min^{1/2}$) was a result of the Zn^{2+} ions diffusion through the boundary layer (film) that surrounds the NaOH-activated CGD biochar particles, to achieve the external surface of the biochar. After that, the superficial diffusion (intraparticle diffusion) of Zn^{2+} ions into the porous system of the biochar took place from 60 to 95 min (approximately 7.5–11 $min^{1/2}$). Worch (2012) reported that intraparticle diffusion occurs primarily in macropores (>50 nm) and mesopores (2–50 nm), while micropore volume (<2 nm) is responsible for the adsorption [46]. The final stages of Zn^{2+} adsorption were a slowdown in diffusion which occurred after 95 min (11 $min^{1/2}$). The decrease in diffusion was caused by the low concentration of adsorbate in the solution [47] and the porous system (macrospores and mesopores) filling with an adsorbate. Thus, the diffusion of Zn^{2+} on the various biochars depends not only on the structure of the adsorbent but also on the concentration of the adsorbate in the solution.

3.4. Adsorption isotherms

The models of Langmuir, Freundlich, Temkin and Dubinin–Radushkevich were used to study the isotherm experimental data of Zn(II) adsorption on NaOH-activated CGD biochar and coffee grounds (CG). The adsorption isotherm parameters obtained are shown in Table 6. As shown in Table 6, all models show an R^2 value greater than 0.9; therefore, these models can better describe the Zn(II) adsorption on NaOH-activated CGD biochar and coffee grounds (CG). The result, 0 < k_L < 1, after adjustment by Langmuir,

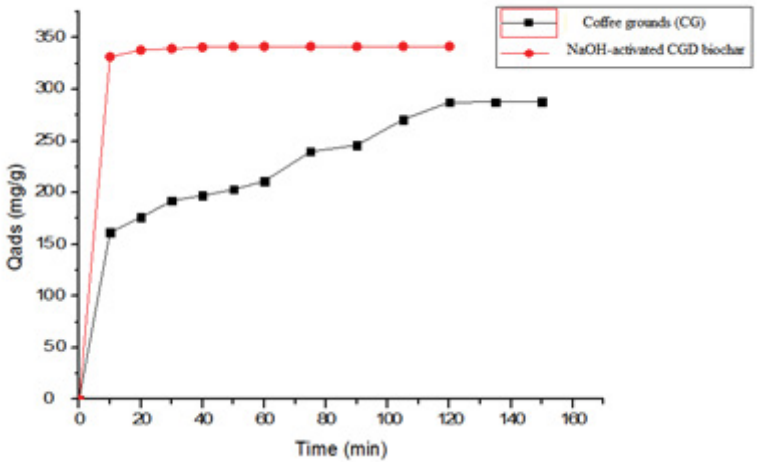

Fig. 3. Kinetics study of Zn on coffee grounds and NaOH-activated CGD biochar.

Table 5
Kinetic parameters for Zn^{2+} adsorption on CG and NaOH-activated CGD biochar

Adsorbents	$Q_{e,exp}$ (μmol g^{-1})	Pseudo-first-order			Pseudo-second-order		
		Q_e (μmol g^{-1})	k_1 (min^{-1})	R^2	Q_e	k_2 (g mg^{-1} min^{-1})	R^2
NaOH-activated CGD biochar	338.4	115.8	0.6	0.72	248.1	0.6	0.99
Coffee grounds (CG)	259.2	325.1	0.7	0.97	338.4	0.040	0.99

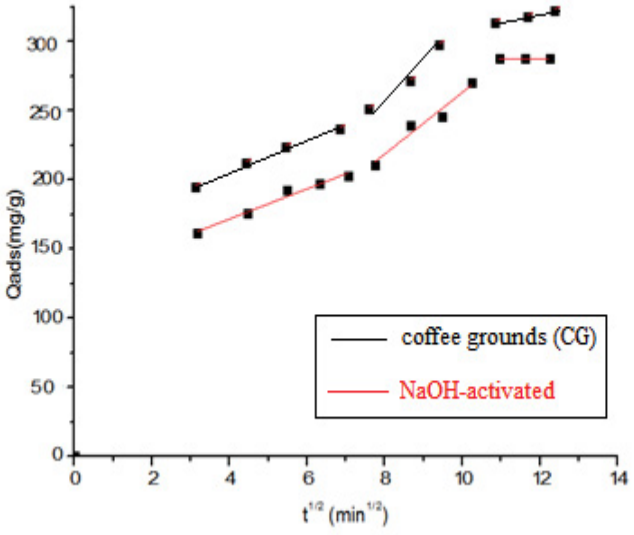

Fig. 4. Intraparticle diffusion of Zn^{2+} adsorbed on the NaOH-activated CGD biochar.

further indicates that the Zn(II) was easily adsorbed by the two adsorbents.

3.5. Thermodynamic study

The thermodynamic experiments were carried out under temperature conditions of 303, 313, 333 and 353 K respectively. The corresponding thermodynamic parameters are shown in Table 7. The negative ΔH value indicates that the adsorption of Zn(II) on NaOH-activated biochar CGD is exothermic. The negative ΔG value indicates that the adsorption reaction of Zn(II) on biochar CGD activated by NaOH is spontaneous [48].

The entropy is a physical parameter that informs us about the order of a reaction. Here the negative value of entropy means that something is becoming less disordered. For something to become less disordered, energy must be used. This will not occur spontaneously [49].

In this study, the adsorption capacity of NaOH-activated CGD biochar was compared with various adsorbents. The maximum adsorption capacities of the different adsorbents are shown in Table 8.

Table 6
Isotherm parameters for wastewater studied sorption on CG and NaOH-activated CGD biochar for Zn

Model	Langmuir			Freundlich			Temkin			Dubinin–Radushkevich		
Constant	R^2	k_L (L mg^{-1})	Q_m	R^2	k_F (mg g^{-1} (L $mg^{-1})^{1/n}$)	n_F	R^2	B_T	k_T (L mg^{-1})	R^2	E (kJ mol^{-1})	Q_{max} (μmol g^{-1})
Coffee grounds (CG)	0.95	0.50	300.51	0.932	13.67	3.49	0.938	5.587	9.395	0.957	2.832	360.53
NaOH-activated CGD biochar	0.98	0.722	680.2	0.96	15.30	4.6	0.95	6.844	9.876	0.97	2.872	220.32

Table 7
Thermodynamic parameters obtained for Zn adsorption on NaOH-activated CGD biochar

T (°C)	ΔG° (kJ mol^{-1})	ΔH° (kJ mol^{-1})	ΔS° (J mol^{-1} K^{-1})	R^2
303	–11.498	–23.740	–43.608	0.987
313	–11.284			
333	–9.012			
353	–8.005			

Table 8
Maximum Zn^{2+} adsorption capacities of the different adsorbents

Adsorbent	Maximum adsorption capacities of Zn^{2+} (μmol g^{-1})	References
Hardwood	6.79	[50]
Corn straw	11.00	[50]
Pine biochar	1	[51]
Jarrah biochar	2.31	[51]
Activated carbon	3.93	[51]
Green cedar biochar	0.396	[52]
Waste compost biochar	0.426	[52]
Pistachio shell biochar	0.353	[52]
NaOH-activated CGD biochar	338.4	This work

NaOH-activated CGD biochar has a high adsorption capacity compared to other adsorbents presented in Table 8. Therefore, considering the low cost of this natural adsorbent (waste), it can be used as an alternative material to minimize the concentration of Zn(II) in wastewater.

4. Conclusions

The NaOH-activated carbon produced from coffee grounds (CG) had a high specific surface area. Kinetic models indicate that the Zn(II)/activated carbon system was best described by pseudo-second-order models and all isotherm models described the adsorption system. The prepared NaOH-activated carbon showed a high adsorption capacity of 340 mg g^{-1} compared to coffee grounds (CG) (300.51 mg g^{-1}). Therefore, coffee grounds (CG) could be considered as a potential precursor for the production of activated carbon, which has great potential to adsorb Zn(II) from aqueous solutions.

References

[1] P. Maneechakr, S. Mongkollertlop, Investigation on adsorption behaviors of heavy metal ions (Cd^{2+}, Cr^{3+}, Hg^{2+} and Pb^{2+}) through low-cost/active manganese dioxide-modified magnetic biochar derived from palm kernel cake residue, J. Environ. Chem. Eng., 8 (2020) 104467, doi: 10.1016/j.jece.2020.104467.

[2] J. Mabrouki, G. Fattah, N. Al-Jadabi, Y. Abrouki, D. Dhiba, M. Azrour, S. El Hajjaji, Study, simulation and modulation of solar thermal domestic hot water production systems, Model. Earth Syst. Environ., (2021) 1–10, doi: 10.1007/s40808-021-01200-w.

[3] Y. Feng, P. Liu, Y. Wang, Y.Z. Finfrock, X. Xie, C. Su, N. Liu, Y. Yang, Y. Xu, Distribution and speciation of iron in Fe-modified biochars and its application in removal of As(V), As(III), Cr(VI), and Hg(II): an X-ray absorption study, J. Hazard. Mater., 384 (2020) 121342, doi: 10.1016/j.jhazmat.2019.121342.

[4] J. Mabrouki, A. Moufti, I. Bencheikh, K. Azoulay, Y. El Hamdouni, S. El Hajjaji, Optimization of the Coagulant Flocculation Process for Treatment of Leachate of the Controlled Discharge of the City Mohammedia (Morocco), International Conference on Advanced Intelligent Systems for Sustainable Development, Springer, Cham, 2019, pp. 200–212.

[5] H. Li, X. Dong, E.B. da Silva, L.M. de Oliveira, Y. Chen, L.Q. Ma, Mechanisms of metal sorption by biochars: biochar characteristics and modifications, Chemosphere, 178 (2017) 466–478.

[6] Y. Deng, S. Huang, D.A. Laird, X. Wang, Z. Meng, Adsorption behaviour and mechanisms of cadmium and nickel on rice straw biochars in single- and binary-metal systems, Chemosphere, 218 (2019) 308–318.

[7] F. Ghorbani, S. Kamari, S. Zamani, S. Akbari, M. Salehi, Optimization and modeling of aqueous Cr(VI) adsorption onto activated carbon prepared from sugar beet bagasse agricultural waste by application of response surface methodology, Surf. Interfaces, 18 (2020) 100444, doi: 10.1016/j.surfin.2020.100444.

[8] M.D. Yahya, K.S. Obayomi, M.B. Abdulkadir, Y.A. Iyaka, A.G. Olugbenga, Characterization of cobalt ferrite-supported activated carbon for removal of chromium and lead ions from tannery wastewater via adsorption equilibrium, Water Sci. Eng., 13 (2020) 202–213.

[9] S. Afroze, T.K. Sen, A review on heavy metal ions and dye adsorption from water by agricultural solid waste adsorbents, Water Air Soil Pollut., 229 (2018) 225, doi: 10.1007/s11270-018-3869-z.

[10] P. Sherugar, N.S. Naik, M. Padaki, V. Nayak, A. Gangadharan, A.R. Nadig, S. Déon, Fabrication of zinc doped aluminium oxide/polysulfone mixed matrix membranes for enhanced antifouling property and heavy metal removal, Chemosphere, 275 (2021) 130024, doi: 10.1016/j.chemosphere.2021.130024.

[11] H. Zhu, J. Yuan, X. Tan, W. Zhang, M. Fang, X. Wang, Efficient removal of Pb^{2+} by Tb-MOFs: identifying the adsorption mechanism through experimental and theoretical investigations, Environ. Sci. Nano, 6 (2019) 261–272.

[12] M. Rahmani, J. Mabrouki, B. Regraguy, A. Moufti, M. El'Mrabet, A. Dahchour, S. El Hajjaji, Adsorption of (methylene blue) onto natural oil shale: kinetics of adsorption, isotherm and thermodynamic studies, Int. J. Environ. Anal. Chem., (2021) 1–15, doi: 10.1080/03067319.2021.1957466.

[13] K. Azoulay, I. Bencheikh, J. Mabrouki, N. Samghouli, A. Moufti, A. Dahchour, S. El Hajjaji, Adsorption mechanisms of azo dyes binary mixture onto different raw palm wastes, Int. J. Environ. Anal. Chem., (2021) 1–20, doi: 10.1080/03067319.2021.1878165.

[14] I. Bencheikh, K. Azoulay, J. Mabrouki, S. El Hajjaji, A. Moufti, N. Labjar, The use and the performance of chemically treated artichoke leaves for textile industrial effluents treatment, Chem. Data Collect., 31 (2021) 100597, doi: 10.1016/j.cdc.2020.100597.

[15] K. Azoulay, I. Bencheikh, A. Moufti, A. Dahchour, J. Mabrouki, S. El Hajjaji, Comparative study between static and dynamic adsorption efficiency of dyes by the mixture of palm waste using the central composite design, Chem. Data Collect., 27 (2020) 100385, doi: 10.1016/j.cdc.2020.100385.

[16] Y. Abrouki, J. Mabrouki, A. Anouzla, S.K. Rifi, Y. Zahiri, S. Nehhal, A. El Yadini, R. Slimani, S. El Hajjaji, H. Loukili, S. Souabi, Optimization and modeling of a fixed-bed biosorption of textile dye using agricultural biomass from the Moroccan Sahara, Desal. Water Treat., 240 (2021) 144–151.

[17] N. Javid, A. Nasiri, M. Malakootian, Removal of nonylphenol from aqueous solutions using carbonized date pits modified with ZnO nanoparticles, Desal. Water Treat., 141 (2019) 140–148.

[18] M.M. Meimand, N. Javid, M. Malakootian, Adsorption of sulfur dioxide on clinoptilolite/nano iron oxide and natural clinoptilolite, Health Scope J., 8 (2019) e69158, doi: 10.5812/jhealthscope.69158.
[19] H. Loukili, J. Mabrouki, A. Anouzla, Y. Kouzi, S.A. Younssi, K. Digua, Y. Abrouki, Pre-treated Moroccan natural clays: application to the wastewater treatment of textile industry, Desal. Water Treat., 240 (2021) 124–136.
[20] P.K. Malik, Dye removal from wastewater using activated carbon developed from sawdust: adsorption equilibrium and kinetics, J. Hazard. Mater., 113 (2004) 81–88.
[21] B. Regraguy, M. Rahmani, J. Mabrouki, F. Drhimer, I. Ellouzi, C. Mahmou, A. Dahchour, M. El Mrabet, S. El Hajjaji, Photocatalytic degradation of methyl orange in the presence of nanoparticles $NiSO_4/TiO_2$, Nanotechnol. Environ. Eng., 7 (2022) 157–171.
[22] A.L. Cazetta, A.M.M. Vargas, E.M. Nogami, M.H. Kunita, M.R. Guilherme, A.C. Martins, T.L. Silva, J.C.G. Moraes, V.C. Almeida, NaOH-activated carbon of high surface area produced from coconut shell: kinetics and equilibrium studies from the methylene blue adsorption, Chem. Eng. J., 174 (2011) 117–125.
[23] J. Rizhikovs, J. Zandersons, B. Spince, G. Dobele, E. Jakab, Preparation of granular activated carbon from hydrothermally treated and pelletized deciduous wood, J. Anal. Appl. Pyrolysis, 93 (2012) 68–76.
[24] T. Rachiq, J. Mabrouki, S. El Hajjaji, S. Rahal, Simulation of the Treatment Performance of a Purification Plant for a Dairy Effluent, M. Azrour, A. Irshad, R. Chaganti, Eds., IoT and Smart Devices for Sustainable Environment, EAI/Springer Innovations in Communication and Computing, Springer, Cham, 2022, pp. 19–27.
[25] B. Alhayani, A.A. Abdallah, Manufacturing intelligent Corvus corone module for a secured two way image transmission under WSN, Eng. Comput., 38 (2020) 1751–1788.
[26] B.S.A. Alhayani, H. llhan, Visual sensor intelligent module based image transmission in industrial manufacturing for monitoring and manipulation problems, J. Intell. Manuf., 32 (2021) 597–610.
[27] H. Sabah Hasan, A.A. Abdallah, I. Khan, H. Sadek Alosman, A. Kolemen, B. Alhayani, Novel unilateral dental expander appliance (UDEX): a compound innovative materials, CMC-Comput. Mater. Continua, 68 (2021) 3499–3511.
[28] A. Farsi, N. Javid, M. Malakootian, Investigation of adsorption efficiency of Cu^{2+} and Zn^{2+} by red soil and activated bentonite from acid copper mine drainage, Desal. Water Treat., 144 (2019) 172–184.
[29] N. Azouaou, Z. Sadaoui, A. Djaafri, H. Mokaddem, Adsorption of cadmium from aqueous solution onto untreated coffee grounds: equilibrium, kinetics and thermodynamics, J. Hazard. Mater., 184 (2010) 126–134.
[30] Z. Honarmandrad, N. Javid, M. Malakootian, Efficiency of ozonation process with calcium peroxide in removing heavy metals (Pb, Cu, Zn, Ni, Cd) from aqueous solutions, SN Appl. Sci., 2 (2020) 703, doi: 10.1007/s42452-020-2392-1.
[31] S. Norouzi, M. Heidari, V. Alipour, O. Rahmanian, M. Fazlzadeh, F. Mohammadi-Moghadam, H. Nourmoradi, B. Goudarzi, K. Dindarloo, Preparation, characterization and Cr(VI) adsorption evaluation of NaOH-activated carbon produced from Date Press Cake; an agro-industrial waste, Bioresour. Technol., 258 (2018) 48–56.
[32] T. Rachiq, Y. Abrouki, J. Mabrouki, N. Samghouli, C. Fersi, S. Rahal, S. El Hajjaji, Evaluation of the efficiency of different materials to remove specific pollutants from landfill leachate, Desal. Water Treat., (2021) 1–11, doi: 10.5004/dwt.2021.27779.
[33] P. Jiao, X. Zhang, N. Li, Y. Wei, P. Wang, P. Yang, Cooperative adsorption of L-tryptophan and sodium ion on a hyper-cross-linked resin: experimental studies and mathematical modeling, J. Chromatogr. A, 1648 (2021) 462211, doi: 10.1016/j.chroma.2021.462211.
[34] J. Gao, Z. Du, Q. Zhao, Y. Guo, F. Cheng, Enhanced Li+ adsorption by magnetically recyclable iron-doped lithium manganese oxide ion-sieve: synthesis, characterization, adsorption kinetics and isotherm, J. Mater. Res. Technol., 13 (2021) 228–240.
[35] M.A. Al-Ghouti, D.A. Da'ana, Guidelines for the use and interpretation of adsorption isotherm models: a review, J. Hazard. Mater., 393 (2020) 122383, doi: 10.1016/j.jhazmat.2020.122383.
[36] W. Wang, X. Zhang, Y. Zhang, X. Mi, R. Wang, H. Shi, C. Li, Z. Du, Y. Qiao, Adsorption of emerging sodium p-perfluorous nonenoxybenzene sulfonate (OBS) onto soils: kinetics, isotherms and mechanisms, Pedosphere, 31 (2021) 596–605.
[37] A.C. Martins, O. Pezoti, A.L. Cazetta, K.C. Bedin, D.A.S. Yamazaki, G.F.G. Bandoch, T. Asefa, J.V. Visentainer, V.C. Almeida, Removal of tetracycline by NaOH-activated carbon produced from macadamia nut shells: kinetic and equilibrium studies, Chem. Eng. J., 260 (2015) 291–299.
[38] G. Fan, C. Zhang, T. Wang, J. Deng, Y. Cao, L. Chang, G. Zhou, Y. Wu, P. Li, New insight into surface adsorption thermodynamic, kinetic properties and adsorption mechanisms of sodium oleate on ilmenite and titanaugite, Adv. Powder Technol,. 31 (2020) 3628–3639.
[39] J. Mabrouki, M. Benbouzid, D. Dhiba, S. El Hajjaji, Simulation of wastewater treatment processes with Bioreactor Membrane Reactor (MBR) treatment versus conventional the adsorbent layer-based filtration system (LAFS), J. Environ. Anal. Chem., (2020) 1–11, doi: 10.1080/03067319.2020.1828394.
[40] K. Kaikake, K. Hoaki, H. Sunada, R.P. Dhakal, Y. Baba, Removal characteristics of metal ions using degreased coffee beans: adsorption equilibrium of cadmium(II), Bioresour. Technol., 98 (2007) 2787–2791.
[41] R. Ahmad, R. Kumar, Adsorption studies of hazardous malachite green onto treated ginger waste, J. Environ. Manage., 91 (2010) 1032–1038.
[42] F. Hanum, R.J. Gultom, M. Simanjuntak, Adsorpsi Zat Warna Metilen Biru dengan Karbon Aktif dari Kulit Durian Menggunakan KOH dan NAOH sebagai Aktivator, Jurnal Teknik Kimia USU, 6 (2017) 49–55.
[43] N.A.H.M. Zaidi, L.B.L. Lim, A. Usman, *Artocarpus odoratissimus* leaf-based cellulose as adsorbent for removal of methyl violet and crystal violet dyes from aqueous solution, Cellulose, 25 (2018) 3037–3049.
[44] D. Jiang, Y. Yang, C. Huang, M. Huang, J. Chen, T. Rao, X. Ran, Removal of the heavy metal ion nickel(II) via an adsorption method using flower globular magnesium hydroxide, J. Hazard. Mater., 373 (2019) 131–140.
[45] K. Foo, B. Hameed, Textural porosity, surface chemistry and adsorptive properties of durian shell derived activated carbon prepared by microwave assisted NaOH activation, Chem. Eng. J., 187 (2012) 53–62.
[46] E. Worch, Adsorption Technology in Water Treatment: Fundamentals, Processes, and Modeling, Walter de Gruyter, 2012.
[47] W. Cheung, Y. Szeto, G. McKay, Intraparticle diffusion processes during acid dye adsorption onto chitosan, Bioresour. Technol., 98 (2007) 2897–2904.
[48] A.M. Osman, A.H. Hendi, T.A. Saleh, Simultaneous adsorption of dye and toxic metal ions using an interfacially polymerized silica/polyamide nanocomposite: kinetic and thermodynamic studies, J. Mol. Liq., 314 (2020) 113640, doi: 10.1016/j.molliq.2020.113640.
[49] L. del Rio, J. Åberg, R. Renner, O. Dahlsten, V. Vedral, The thermodynamic meaning of negative entropy, Nature, 474 (2011) 61–63.
[50] X. Chen, G. Chen, L. Chen, Y. Chen, J. Lehmann, M.B. McBride, A.G. Hay, Adsorption of copper and zinc by biochars produced from pyrolysis of hardwood and corn straw in aqueous solution, Bioresour. Technol., 102 (2011) 8877–8884.
[51] S. Jiang, L. Huang, T.A. Ok, Y.S. Nguyen, V. Rudolph, H. Yang, D. Zhang, Copper and zinc adsorption by softwood and hardwood biochars under elevated sulphate-induced salinity and acidic pH conditions, Chemosphere, 142 (2016) 64–71.
[52] A. Rodríguez-Vila, H. Selwyn-Smith, L. Enunwa, I. Smail, E.F. Covelo, T. Sizmur, Predicting Cu and Zn sorption capacity of biochar from feedstock C/N ratio and pyrolysis temperature, Environ. Sci. Pollut. Res., 25 (2018) 7730–7739.